Theor. Comput. Fluid Dyn. (2010) 24:45–50
DOI 10.1007/s00162-009-0174-x

ORIGINAL ARTICLE

Scott David Kelly · Hailong Xiong

Self-propulsion of a free hydrofoil with localized discrete vortex shedding: analytical modeling and simulation

Received: 10 November 2008 / Accepted: 24 September 2009 / Published online: 2 March 2010

Abstract We present a model for the self-propulsion of a free deforming hydrofoil in a planar ideal fluid. We begin with the equations of motion for a deforming foil interacting with a pre-existing system of point vortices and demonstrate that these equations possess a Hamiltonian structure. We add a mechanism by which new vortices can be shed from the trailing edge of the foil according to a time-periodic Kutta condition, imparting thrust to the foil such that the total impulse in the system is conserved. Simulation of the resulting equations reveals at least qualitative agreement with the observed dynamics of fishlike locomotion. We conclude by comparing the energetic properties of two distinct turning gaits for a free Joukowski foil with varying camber.

Keywords Aquatic locomotion · Noncanonical Hamiltonian systems

1 Introduction

Recent study by the authors and others has addressed two complementary problems in fluid-body interactions from the standpoint of analytical mechanics. The self-propulsion of a deformable body in an ideal fluid devoid of vorticity is treated as a problem in Lagrangian mechanics in [1–3] and related articles. Parallels between this problem and locomotion at low Reynolds number are detailed in [2,3]; the addition of liftlike forces due to circulation is described in [4]. Hamiltonian models for the interactions of free rigid bodies with discrete vortex structures are presented, meanwhile, in [5–9]. In the present article, a summary of work detailed in [10], we merge these lines of research to provide a model for the self-propulsion of a deformable body in a planar ideal fluid—specifically, a hydrofoil defined by a time-varying conformal map—which is able to shed vorticity discretely from a single point on its surface in accordance with a periodically applied Kutta condition. The shedding of each vortex is accompanied by the application of an impulsive force to the hydrofoil to conserve the total impulse in the system. Between vortex shedding events, the equations of motion possess a Hamiltonian structure which extends that underpinning the interaction of a free rigid body with a system of vortices. Computational experiments with this model demonstrate its qualitative fidelity to biological and robotic fishlike locomotion.

Communicated by H. Aref

S. D. Kelly(✉)
Department of Mechanical Engineering and Engineering Science, University of North Carolina at Charlotte, Charlotte, NC, USA
E-mail: scott@kellyfish.net

H. Xiong
Quantitative Risk Management Inc., Chicago, IL, USA
E-mail: xiong@snapturn.com

Undulatory fishlike locomotion has inspired designs for manmade aquatic vehicles since the eighteenth century or before [11], yet the control of such devices remains largely an empirical science due to the scarcity of mathematical models that exhibit sufficient fidelity to the relevant physics, under a sufficient diversity of circumstances, without exceeding the formal scope of model-based control theory. High-fidelity models for fishlike locomotion are almost universally computational in nature; contemporary approaches to control design require analytical models. The present article addresses this divide by framing a mechanism central to fishlike locomotion—the development of thrust through localized vortex shedding from the caudal fin—in a Hamiltonian setting. Although rooted in conservative mechanics, the model described herein embodies the same principle of momentum balance that governs aquatic locomotion in a truly viscous fluid, and illuminates the structure of propulsive wakes corresponding to diverse swimming gaits.

2 Modeling

We model the contour of a hydrofoil with time-varying shape as the image of a circle in the complex plane under a conformal map $z = x + iy = F(\zeta)$ with time-varying parameters s_j. We require the area within the foil to remain constant in time to avoid an infinite term in the kinetic energy of the resulting fluid–foil system. We express the dynamics of the moving foil relative to the foil-fixed z-frame. In between vortex shedding events, the flow resulting from the motion of the foil and vortices—assuming the fluid to be at rest infinitely far away, and excluding small domains around the vortices themselves—is determined by a potential function of the form

$$W(z) = w(\zeta) = U w_1(\zeta) + V w_2(\zeta) + \Omega w_3(\zeta) + \sum_j \dot{s}_j w_{s_j}(\zeta) + \sum_k w_{v_k}(\zeta), \tag{1}$$

where U and V are the x- and y-components of the foil's translational velocity, Ω is its angular velocity, and the complex potentials w_{v_k} represent the contributions of the vortices to the flow.

Relative to the foil-fixed frame, the total linear and angular impulse in the fluid–foil system may be expressed in the form

$$\begin{bmatrix} L_x \\ L_y \\ P \end{bmatrix} = I(\mathbf{s})\xi + B(\mathbf{s})\dot{\mathbf{s}} + \sum_k \gamma_k K_k(\mathbf{s}, z_k), \tag{2}$$

where $\mathbf{s}$ is the vector of shape parameters for the foil, γ_k and z_k are the strength and location of the kth vortex, $I(\mathbf{s})$ and $B(\mathbf{s})$ are shape-dependent matrices with appropriate dimensions, and $\xi = [U\ V\ \Omega]^T$. The motion of the foil is governed by *Kirchhoff's equations*

$$\left(\frac{\mathrm{d}}{\mathrm{d}t} + \bar{\Omega}\times\right)\mathbf{L} = 0, \quad \frac{\mathrm{d}\mathbf{P}}{\mathrm{d}t} + \mathbf{U}\times\mathbf{L} = 0, \tag{3}$$

where $\bar{\Omega} = [0\ 0\ \Omega]^T$, $\mathbf{L} = [L_x\ L_y\ 0]^T$, $\mathbf{P} = [0\ 0\ P]^T$, and $\mathbf{U} = [U\ V\ 0]^T$. The motion of the kth vortex is determined using *Routh's rule* [12] such that

$$\dot{\zeta}_k = \left(\overline{\frac{\mathrm{d}W_k}{\mathrm{d}z}} - (U + iV + i\Omega z_k) - \sum_j \frac{\partial F}{\partial s_j}\dot{s}_j\right)\frac{1}{F'(\zeta_k)}, \tag{4}$$

where $W_k(z) = W(z) - i\gamma_k \log(z - z_k)$.

Observing that

$$I(\mathbf{s})\xi = \begin{bmatrix} L_x \\ L_y \\ P \end{bmatrix} - B(\mathbf{s})\dot{\mathbf{s}} - \begin{bmatrix} \int \mathbf{l}\times(\mathbf{n}\times\nabla\phi_v)\mathrm{d}s \\ -\frac{1}{2}\int l^2(\mathbf{n}\times\nabla\phi_v)\mathrm{d}s \end{bmatrix} - \sum_k(-2\pi\gamma_k)\begin{bmatrix} y_k \\ -x_k \\ -\frac{1}{2}(x_k^2 + y_k^2) \end{bmatrix} \tag{5}$$

in the notation of [7], we may define the Hamiltonian function

$$H(L_x, L_y, P, x_1, y_1, \ldots, x_N, y_N) = \frac{1}{2}\xi^T I(\mathbf{s})\xi - 2\pi H_1 \tag{6}$$

when N wake vortices are present, where

$$H_1 = \sum_k \gamma_k \sum_j \dot{s}_j \psi_{s_j}(x_k, y_k) - \frac{1}{2}\sum_k \gamma_k^2 \left(\log\left|\zeta_k\overline{\zeta_k} - r_c^2\right| + \log\left|F'(\zeta_k)\right|\right)$$
$$+\frac{1}{2}\sum_k \sum_{j\neq k} \gamma_k\gamma_j \left(\log\left|\zeta_k - \zeta_j\right| - \log\left|\zeta_k\overline{\zeta_j} - r_c^2\right|\right). \tag{7}$$

If $\mu = [L_x \; L_y \; P]^T$, then the motion of the foil is governed in between vortex shedding events by the *Lie–Poisson equations*

$$\dot{\mu} = \mathrm{ad}^*_{\delta H/\delta\mu}\mu \tag{8}$$

on $\mathfrak{se}^*(2)$ [13], while the positions of the vortices evolve such that

$$(-2\pi\gamma_k)\frac{\mathrm{d}x_k}{\mathrm{d}t} = \frac{\partial H}{\partial y_k}, \quad (-2\pi\gamma_k)\frac{\mathrm{d}y_k}{\mathrm{d}t} = -\frac{\partial H}{\partial x_k}. \tag{9}$$

We introduce new vortices to the wake near the trailing edge of the foil in simultaneous accord with the conservation of impulse and the Kutta condition. This leaves flexibility in the way in which we select the (coupled) position and strength of each new vortex. We provide a comparison of different methods for doing so in [10], and settle on a method described in [14] for the present discussion. According to this method, we situate each new vortex along a contour interpolated from the trailing edge of the foil to the current position of the last vortex shed, and determine the strength of each new vortex as a function of its initial position. Vortices shed at different times may have different strengths; the strength of each shed vortex is assumed to remain constant thereafter. Enforcing the constraints described above, we introduce each vortex with strength γ_k at the image of the point ζ_k such that

$$\left.\frac{\mathrm{d}w}{\mathrm{d}\zeta}\right|_{\zeta=\zeta_T} = 0, \tag{10}$$

where ζ_T is the pre-image of the trailing edge of the foil under the transformation defining the foil's shape, and such that

$$I(\mathbf{s})\,\Delta\xi + \gamma_k K_k(\mathbf{s}, z_k) = 0, \tag{11}$$

where $\Delta\xi$ refers to the impulsive change in the foil's linear and angular velocity as a result of shedding.

We note that this method for introducing new vortices relies on the fact that the complex transformation defining the foil's shape has zero derivative at a particular point on the foil. We also note that shed vortices are guaranteed to appear outside the foil, and not inside, provided the contour of the foil is not deformed to such an extreme that it crosses itself.

3 Simulation

Figure 1 shows results from two different simulations based on our model. The top row portrays the acceleration from rest of a von Mises foil undulating according to periodic variations in two shape parameters which, roughly speaking, prescribe the cyclic propagation of traveling waves along the length of the foil from front to back. Wake vortices are depicted in the snapshot on the left as tiny colored circles; red circles correspond to clockwise vortices and blue circles to counterclockwise vortices. We observe the roll-up of wake vorticity into staggered coherent structures; over time, these assume the form of an inverse Kármán vortex street, consistent with experimental observations of the wakes trailing oscillating foils [15]. The plot on the right compares the predicted x- and y-displacement of the foil-fixed frame over time to that which would be measured were the mechanism for vortex shedding disabled ("*ns*"), underscoring the role played by vortex shedding in thrust development. The bottom row depicts the execution of a *snap turn* by a Joukowski foil, the camber of which is varied rapidly about zero through a single sinusoidal period, providing sufficient momentum for the foil to coast in an oblique direction thereafter.

In the context of fishlike robotic locomotion, our model provides a platform not only for algorithmic motion planning but also for evaluating the energetics of individual maneuvers. The agility, energy efficiency,

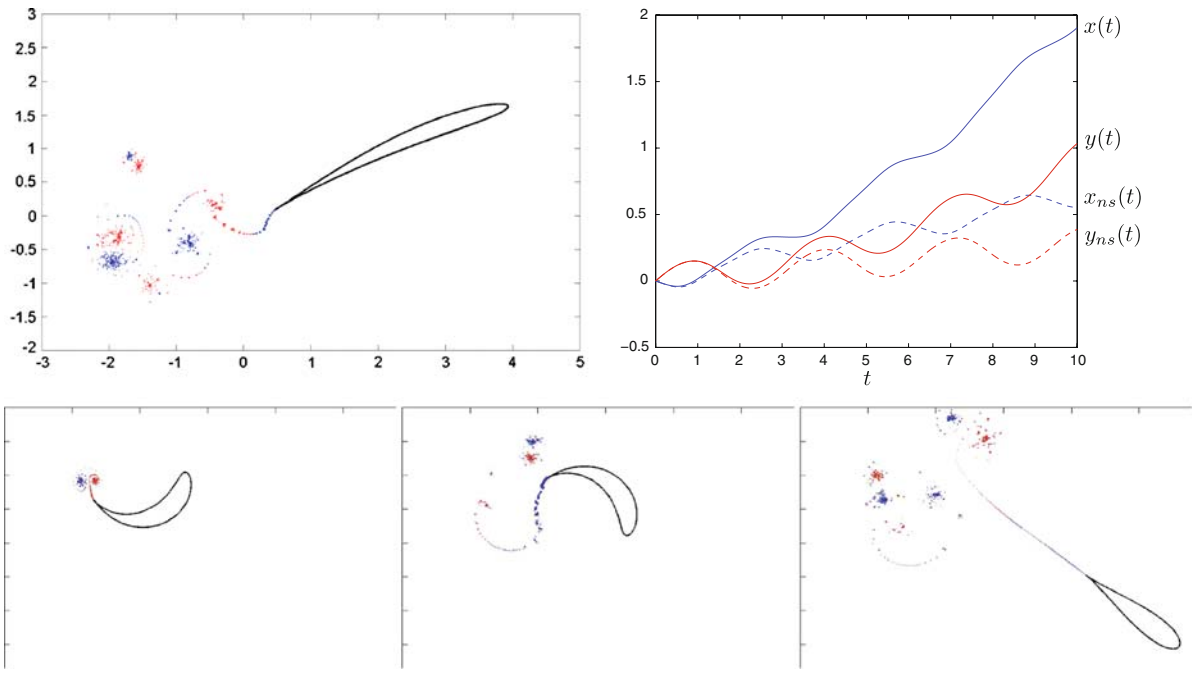

Fig. 1 *Top left*: An undulating von Mises foil sheds vortices as it accelerates from rest. *Top right*: The displacements of the same foil in the x and y directions as functions of time, contrasted with the displacements that would be achieved if the mechanism for vortex shedding were disabled ("*ns*"). *Bottom row*: A Joukowski foil executes a snap turn via an aggressive change in camber

and stealth of marine animals all motivate the study of biological locomotion, but the relationships among these performance metrics are nontrivial. We illustrate a few key distinctions here by contrasting two different turning gaits for a free Joukowski foil with a single internal degree of freedom.

The top two rows of Fig. 2 depict initial, intermediate, and final frames from simulations of these two gaits; the corresponding trajectories of the origin of the foil-fixed frame are depicted at the lower left. The first turn results from eight periodic oscillations in camber superposed with a nonzero bias, the second from two abrupt flicks of the tail to the foil's left.

The Joukowski profile depicted in Fig. 2 is realized as the image of a circle with radius r_c in the ζ plane under a transformation of the form

$$z = \zeta + \zeta_c + \frac{a^2}{(\zeta + \zeta_c)}, \tag{12}$$

where r_c, ζ_c, and a are chosen to vary with time, parametrized by a single shape parameter $s(t)$, to realize area-preserving variations in camber. Neglecting the infinite self-energy of the vortices, the total kinetic energy in the system admits the decomposition

$$\mathrm{KE} = \mathrm{KE}_{\text{due to body motion}} + \mathrm{KE}_{\text{due to vortices}}, \tag{13}$$

where

$$\mathrm{KE}_{\text{due to body motion}} = \frac{1}{2}\begin{bmatrix}\xi^T & \dot{\mathbf{s}}^T\end{bmatrix}\begin{bmatrix} I & B \\ B^T & C\end{bmatrix}\begin{bmatrix}\xi \\ \dot{\mathbf{s}}\end{bmatrix} \tag{14}$$

and

$$\begin{aligned}\mathrm{KE}_{\text{due to vortices}} = &-\sum_k \sum_{j\neq k} \pi\gamma_k\gamma_j \log\left|\zeta_k - \zeta_j\right| + \sum_k \sum_j \pi\gamma_k\gamma_j \log\left|\zeta_k - \zeta_j^*\right| \\ &+\pi\left(\sum_k \gamma_k\right)\left(\sum_k \gamma_k \log\frac{|\zeta_k|}{r_c}\right).\end{aligned} \tag{15}$$

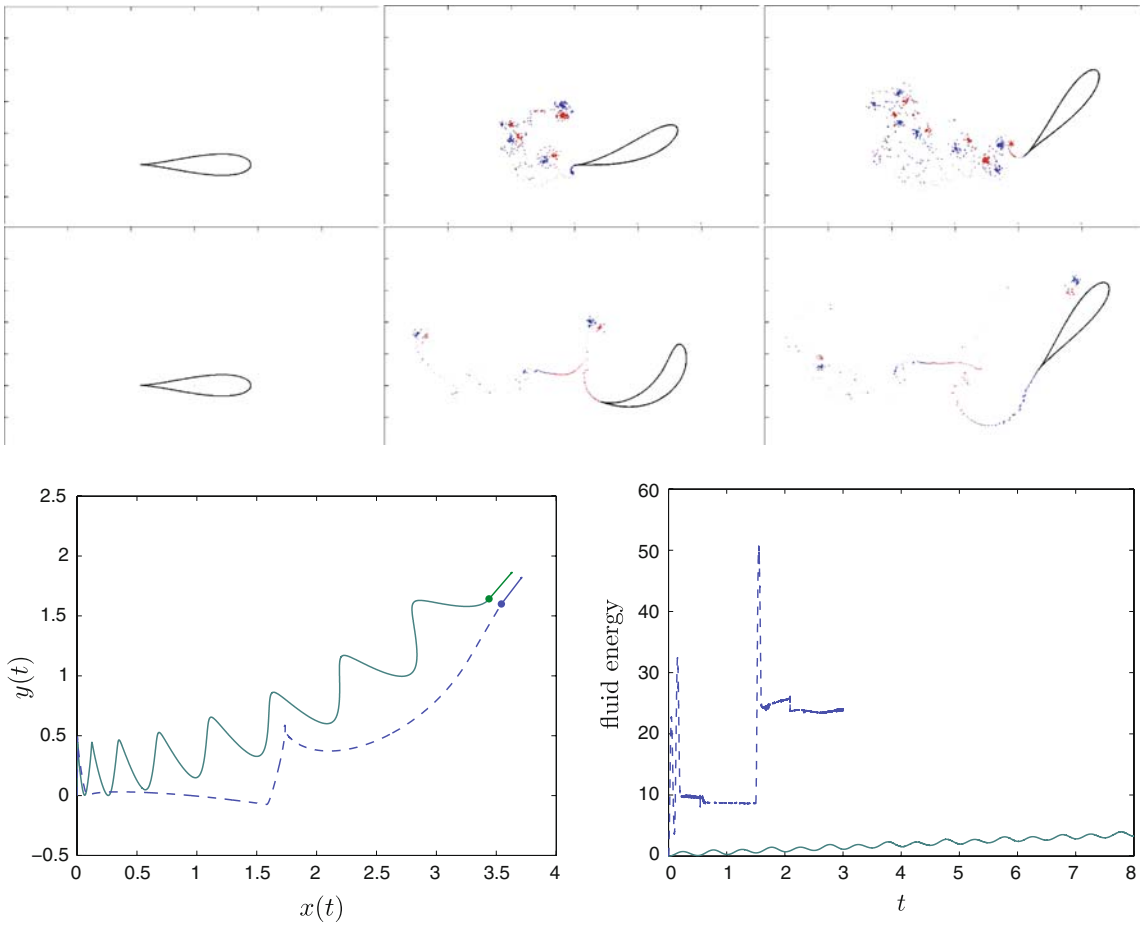

Fig. 2 *Top two rows*: Initial, intermediate, and final snapshots of different turning gaits for a Joukowski foil. *Bottom left*: The trajectories determined in the z plane by these two gaits. *Bottom right*: The fluid energy as a function of time for these two gaits

The plot at the lower right of Fig. 2 depicts the fluid energy—excluding the self-energy of individual vortices—as a function of time through the two different turns shown above.

The control effort

$$E = \frac{1}{2}\int_{t_{\text{initial}}}^{t_{\text{final}}} \dot{s}(t)^2 \mathrm{d}t \tag{16}$$

associated with each of these maneuvers, which may be understood as a measure of economy of motion, is roughly 50% greater in the case of the second turn, which is completed in three-eighths the time required for the first. The energy imparted to the fluid during the second turn, however, is significantly greater. The first turn would arguably be the better choice for a robotic vehicle attempting to escape acoustic detection, the latter the better choice for retreat after being detected.

Acknowledgments Support for this study was provided in part by NSF grants CMMI 04-49319 and ECCS 05-01407.

References

1. Kanso, E., Marsden, J.E., Rowley, C.W., Melli-Huber, J.B.: Locomotion of articulated bodies in a perfect fluid. J. Nonlinear Sci. **15**, 255–289 (2005)
2. Kelly, S.D.: The mechanics and control of robotic locomotion with applications to aquatic vehicles. Ph.D. thesis, California Institute of Technology (1998)

3. Kelly, S.D., Murray, R.M.: The geometry and control of dissipative systems. In: Proceedings of the IEEE Control and Decision Conference (1996)
4. Kelly, S.D., Hukkeri, R.B.: Mechanics, dynamics, and control of a single-input aquatic vehicle with variable coefficient of lift. IEEE Trans. Robot. **22**(6), 1254–1264 (2006)
5. Shashikanth, B.N.: Poisson brackets for the dynamically interacting system of a 2D rigid cylinder and *N* point vortices: the case of arbitrary smooth cylinder shapes. Regul. Chaotic Dyn. **10**(1), 1–14 (2005)
6. Borisov, A.V., Mamaev, I.S., Ramodanov, S.M.: Motion of a circular cylinder and *n* point vortices in an ideal fluid. Regul. Chaotic Dyn. **8**(4), 449–462 (2003)
7. Shashikanth, B.N., Marsden, J.E., Burdick, J.W., Kelly, S.D.: The Hamiltonian structure of a 2-D rigid circular cylinder interacting dynamically with N point vortices. Phys. Fluids **14**, 1214–1227 (2002)
8. Shashikanth, B.N., Sheshmani, A., Kelly, S.D., Marsden, J.E.: Hamiltonian structure for a neutrally buoyant rigid body interacting with N vortex rings of arbitrary shape: the case of arbitrary smooth body shape. Theor. Comput. Fluid Dyn. **22**(1), 37–64 (2008)
9. Shashikanth, B.N., Sheshmani, A., Kelly, S.D., Wei, M.: Hamiltonian Structure and dynamics of a neutrally buoyant rigid sphere interacting with thin vortex rings. J. Math. Fluid Mech. (2008). doi:10.1007/s00021-008-0291-0
10. Xiong, H.: Geometric mechanics, ideal hydrodynamics, and the locomotion of planar shape-changing aquatic vehicles. Ph.D. thesis, University of Illinois at Urbana-Champaign (2007)
11. Richie, J.: Weapons: Designing the Tools of War. Oliver Press, Minneapolis, MN (2000)
12. Saffman, P.G.: Vortex Dynamics. Cambridge University Press, Cambridge (1992)
13. Marsden, J.E., Ratiu, T.S.: Introduction to Mechanics and Symmetry, 2nd edn. Springer, New York (1999)
14. Streitlien, K., Triantafyllou, M.S.: Force and moment on a Joukowski profile in the presence of point vortices. AIAA J. **33**(4), 603–610 (1995)
15. Triantafyllou, M.S., Triantafyllou, G.S.: An efficient swimming machine. Sci. Am. **272**, 64–70 (1995)